JOURNAL OF MATERIALS SCIENCE 32 (1997) 5551–5560

Percolation in magnetic composites‡

T. J. FISKE, H. S. GOKTURK, D. M. KALYON*
Highly Filled Materials Institute, Chemistry and Chemical Engineering Department, Stevens Institute of Technology, Castle Point Station, Hoboken, NJ 07030, USA

Electric and magnetic properties of composite materials consisting of low density polyethylene filled with powdered ferromagnetic materials were investigated‡. The volume fractions of the fillers were varied from 10% up to the theoretical maximum packing fractions, i.e. between 0.70 and 0.77, so that the percolation phenomenon could be investigated. The ferromagnetic fillers used were HyMu 800 (a nickel–iron–molybdenum alloy), MnZn ferrite and NiZn ferrite. The particle sizes and size distributions of the fillers were well characterized by image analysis techniques. Based on the particle size distribution the maximum loading levels of fillers as permitted by geometric considerations were calculated. The properties of the composites characterized included: volume and surface resistivities, dielectric constants, electrical loss factors and magnetic permeabilities.

1. Introduction

The electrically insulating behaviour of most polymers is well documented. The non-conductive nature of polymers together with their ease of processability/shaping into two- or three-dimensional objects is one of the main reasons for their extensive use in the electrical and electronics area. However, there are other applications where electrical conductivity of a shaped article would be desirable. The two principal routes are to use more conductive polymers [1] and/or to use conductive fillers in a polymer matrix [2]. For instance, the shielding of electromagnetic and radio frequency interference (EMI–RFI) necessitates conductive materials [3, 4]. The conductive solid content of the composite can be in the form of powders, flakes or fibres [2]. Various electrically conductive polymers are commercially available [1], but are generally expensive rendering the filler route as the more commonly utilized way of obtaining conductive mouldable materials.

Polymers are inherently non-magnetic. As early as 1955 it was seen that this property could be modified by incorporating magnetic powders in plastic and rubber matrices [5]. The magnetic properties of plastic magnets are generally considered to be inferior to cast and sintered magnets. This is principally related to the relatively low permeability values associated with such composites as opposed to magnetic permeability values of cast and sintered materials. However, polymer composites possess numerous advantages. The polymeric binder coats the magnetic particles and acts as an insulator suppressing eddy current losses [6]. Polymer based magnets can be manufactured using conventional polymer processing techniques; allowing them to be formed into complex shapes and sizes, with higher production rates, lower cost and better uniformity and reproducibility.

This work is part of a larger comprehensive study focusing on the electrical and magnetic properties of polymer/ferromagnetic composites as a function of their constituents. The scope of the project principally includes the evaluation of candidate materials for use at low frequencies. Previously we have reported work on several polymer–ferromagnetic composite systems. By using a thermoplastic elastomer incorporated with ferromagnetic powders (kraton–iron powder and kraton–nickel–iron powder) [7] we were able to show that particle–particle interactions become important above a volume fraction of 0.2. Particle–particle interactions tend to enhance the electrical and magnetic properties. However, the volume fraction used for that study was limited in range and no second-order enhancement of the relative permeability was observed. In another study [8] we examined the effects of particle shapes on the magnetic and electrical properties of low density polyethylene–nickel composite systems. The particles were in the form of spherical powders, filamentary powders, flakes and fibres. Again it was shown that particle–particle interactions influenced the electrical and magnetic properties. As with the previous study, there was no discernible second-order enhancement effect of the relative permeability with volume fraction. In both of the above studies the relative permeability values achieved were $\leqslant 6$. Here, we extend the previous work to include higher quality ferromagnetic fillers and a broader range of volume fraction values.

The objective of this study is to examine the electrical and magnetic properties of a polyethylene–soft ferromagnetic powder composite as a function of the

* Author to whom correspondence should be addressed.
‡ This paper is based on a presentation at the Annual Technical Conference of the Society of Plastic Engineers, New Orleans, LA, May 1993.

0022–2461

volume concentration of the filler, especially at very high loading levels. The volume concentration ranged from 10% (non-interacting particles) all the way up to the theoretical maximum packing fraction.

2. Background

2.1. Resistivity

Resistivity of a polymer composite incorporated with a conductive filler does not decrease linearly with increasing filler content. Instead, the resistivity decreases dramatically over a narrow range of filler concentration. This decrease in resistivity is facilitated by the establishment of conductive paths by the filler particles at a critical filler concentration [1]. Below the critical filler concentration the composite lacks a continuous conductive network and behaves more like the insulating polymer. Above the critical concentration, the composite takes on the characteristics of the conductive filler. Percolation theory has been applied to model this phenomenon and the critical volume concentration at which conductive paths are established, i.e. the percolation threshold, is reported [9].

A simple power law model is often used to describe the percolation phenomenon as [10]

$$R = R_0(\phi - \phi_c)^{-p} \tag{1}$$

where R is the resistivity of the composite, R_0 is the resistivity of the conductive phase, ϕ is the volume fraction of the conductive phase, ϕ_c is the critical volume fraction of the conductive phase, and p is the critical exponent for percolation.

The critical exponent, p, varies with the type of filler. For a system of random packing of spheres p is approximately 1.7 for electrical properties [11]. The percolation limit for electrical properties, ϕ_c, for a dispersion of conductive particles in a continuous medium may range from less than 0.01 for high aspect ratio particles [11] to 0.75 for spherical particles [10].

Finally, it has been shown that the particle size, shape and size distribution [12] as well as the type of material (metal particles can form an oxide layer that increases the contact resistance) [13] all have an effect on the percolation threshold of the electrical properties. The percolation threshold for electrical and magnetic properties are not similar [14].

2.2. Dielectric constant

Due to their usefulness as artificial dielectrics, much time and effort has been expended studying the dielectric properties of composites consisting of conducting particles dispersed in an insulating matrix. The effective permittivity of a composite is a complicated function of the permittivities of the individual components, of the particle size, shape and size distribution, and of the volume loading. Some insight may be gained to this complicated functionality by considering the simple case of a single conductive spherical particle subjected to a uniform external electric field in the z-direction. The analytical solution for the electric field, E, outside the sphere and the surface charge distribution, σ, on the sphere is given by [15]

$$E = E_0\boldsymbol{k} + \left(\frac{a}{r}\right)^3 E_0(2\boldsymbol{U}_r\cos\theta + \boldsymbol{U}_\theta\sin\theta) \tag{2}$$

$$\sigma = 3\varepsilon_0 E_0\cos\theta \tag{3}$$

where E_0 is the external field, a is the radius of the sphere, r and θ are the radial distance and the polar angle in spherical co-ordinates, ε_0 is the permittivity constant, and $\boldsymbol{U}_r$, $\boldsymbol{U}_\theta$ and $\boldsymbol{k}$ represent unit vectors. The first term in Equation 2 is just the applied external field, while the second term represents the contribution of the field due to the presence of the conducting sphere. Notice that the influence of the sphere diminishes inversely with the cube of the radial distance from the centre of the sphere. The surface charge distribution is such that the conducting sphere is polarized like a dipole [15].

It has been shown that a cubic lattice of conducting uniform spherical particles will behave as isolated particles at volume fractions less than 0.2 [7]. The effective permittivity of the composite with non-interacting spherical particles shows a linear relationship with volume concentration as demonstrated by Wagner's equation [16]

$$\varepsilon_{eff} = \varepsilon(1 + 3\phi) \tag{4}$$

where ε is the permittivity of the host matrix, and ϕ is the volume fraction of the filler.

2.3. Magnetic permeability

A similar problem can be formulated for the situation of a single soft magnetic spherical particle subjected to a uniform magnetic field in the z-direction. The analytical solution of the magnetic flux density, B, is [15]

$$B = B_0\boldsymbol{k} + \left(\frac{a}{r}\right)^3 B_0(2\boldsymbol{U}_r\cos\theta + \boldsymbol{U}_\theta\sin\theta) \tag{5}$$

At low volume concentration, the filler can be modelled as isolated non-interacting spheres. Similar to the effective permittivity, the effective magnetic permeability at low densities shows a linear dependence on volume concentration of the filler [16, 17]

$$\mu_{eff} = \mu_0(1 + 3\phi) \tag{6}$$

where μ_{eff} is the effective permeability of the composite, and μ_0 is the permeability constant.

3. Experimental procedure

3.1. Materials

The polymer matrix used in this study was low density polyethylene (LDPE), Petrothene PEV 007 available from USI Chemicals, Cincinnati, OH. Three soft ferromagnetic powdered (low coercivity) fillers were used: one metallic and two ferrites. The metallic ferromagnetic filler used in this study was HyMu 800 procured from Carpenter Technology Corp., Reading, PA. HyMu 800 has a composition (by weight) of 80% nickel, 5% molybdenum, 0.50% manganese, 0.15% silicon, 0.10% carbon and the balance iron. It was supplied in spherical powder form at -100 mesh.

The ferrites were supplied by D. M. Steward MFG Co., Chattanooga, TN. The 28-Material (Steward's designation) is a fully reacted nickel–zinc spinel ferrite powder with a target particle size of 50 μm. The 40-Material (Steward's code) is a fully reacted manganese–zinc spinel ferrite powder. The target particle size for the 40 material was 100 μm.

3.2. Characterization of materials

In order to calculate the maximum packing fraction, ϕ_m, the particle size distributions of the three powders were determined. Samples of the three materials were mounted on sample holders and sputtered with a thin layer of gold. The samples were scanned using a Joel scanning electron microscope at various magnifications of $\times 100$–500. The micrographs obtained (see Fig. 1) were subjected to computerized image analysis techniques. The micrographs were digitized by a frame grabber via a live CCD camera hookup and stored as digital images. These images were then processed with Macintosh IIfx using Image Analyst software procured from Automatix and the particle size distributions were obtained. Based on the particle size distribution, the maximum packing fraction was calculated by the method of Ouchiyama and Tanaka [18, 19]

3.3. Particle size

Figs 2–4 show the particle size distributions of the NiZn ferrite, MnZn ferrite and the HyMu metal as determined by the quantitative image analysis. From Fig. 2 it can be seen that NiZn ferrite exhibits a narrow range of particle sizes, i.e. 50–70 μm. Figs 3 and 4 show that both HyMu metal and MnZn ferrite particles have bimodal size distributions. Based on these determined particle size distributions and assuming spherical particles, the maximum packing fraction values, ϕ_m, where calculated to be 0.671, 0.71 and 0.77 for NiZn ferrite, MnZn ferrite and HyMu metal particles, respectively. The volume fractions of these fillers in polyethylene were varied up to the maximum packing fraction of each.

3.4. Preparation of samples

Mixing the samples of the LDPE–HyMu and LDPE–ferrite composites were prepared in a Haake Rheocord Torque Rheometer, UV5, with a Rheomix 600 mixing head attachment, at 175 °C and 60 r.p.m. The specimens for the electrical measurements were compression moulded into discs that were 76.2 mm in diameter and 6.35 mm in thickness. The surfaces were polished with sandpaper to remove the resin-rich external layer. Contact electrodes were constructed on the surface with Dynaloy 300 conductive silver paint from Zymet in East Hanover, NJ. Toroidal samples with outer diameters of 76.2 mm and inner diameters of 63.5 mm and thicknesses of 6.35 mm were cut from the discs for magnetic permeability measurements. All the samples were prepared using a Carver Glove Box compression moulding press at 175 °C and utilizing moulding pressures of around 10 MPa.

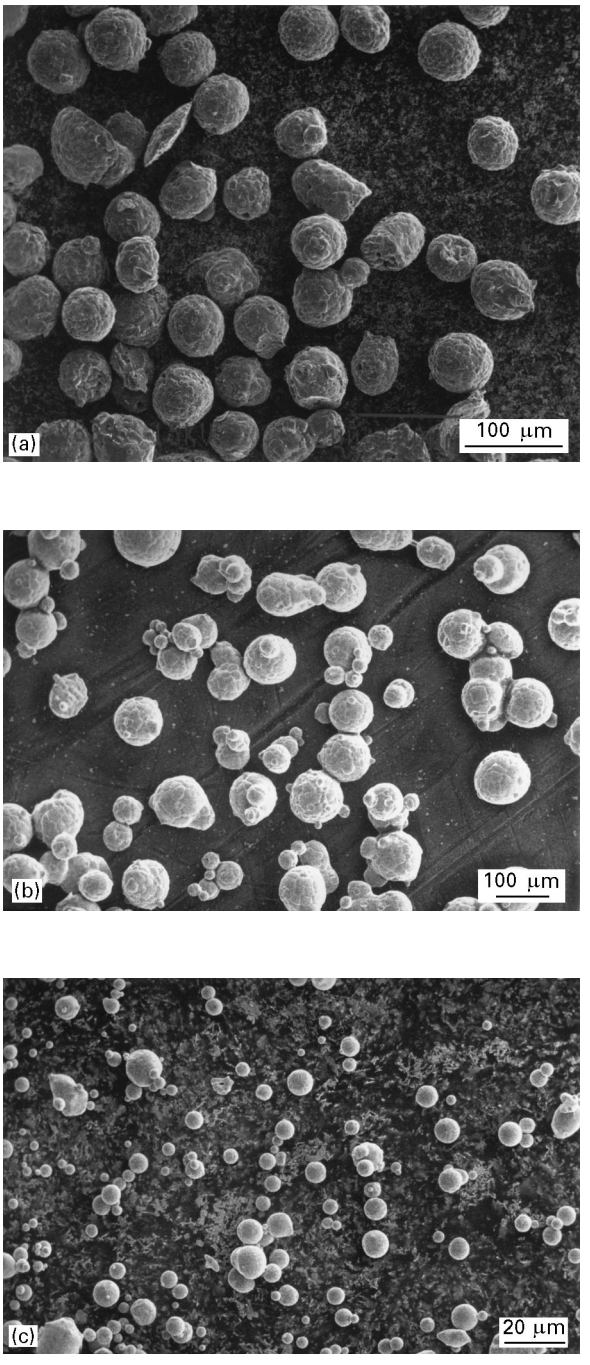

Figure 1 Scanning electron micrographs of filler particles: (a) NiZn ferrite at $\times 140$, (b) MnZn ferrite at $\times 70$, and (c) HyMu metal at $\times 350$ magnification.

3.5. Characterization of electrical properties

The electrical properties measured were the volume and surface resistivity, dielectric constant and electric loss factor. The experimental setup for the volume and surface resistivity measurements consisted of a power supply and a Keithley 485 picoammeter. The basic setup conformed to the ASTM standard designation D257-78. The experimental setup for determining the dielectric constants and electric loss factors consisted of a Hewlett Packard LCR meter model 4284A, a Hewlett Packard dielectric test fixture model 16451B and a Macintosh IIfx computer. The experimental setup conforms to the ASTM standard designation D150-87.

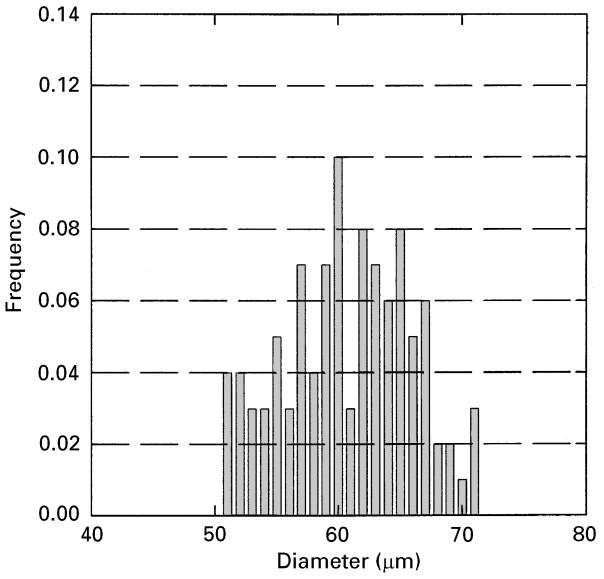

Figure 2 Particle size distribution of NiZn ferrite ($\phi_m = 0.671$).

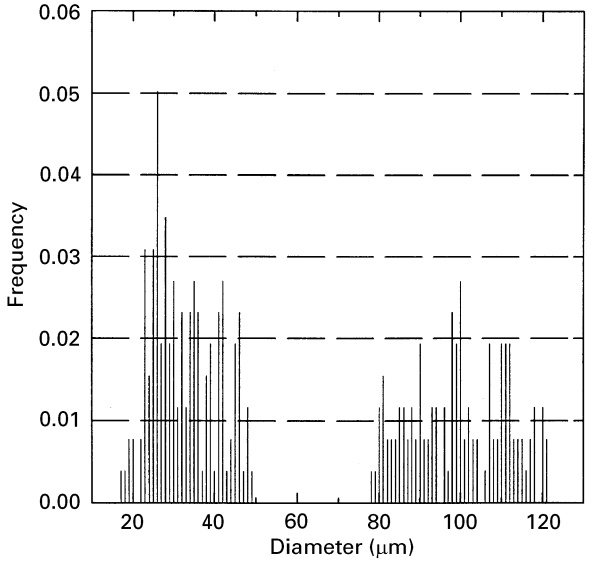

Figure 3 Particle size distribution of MnZn ferrite ($\phi_m = 0.707$).

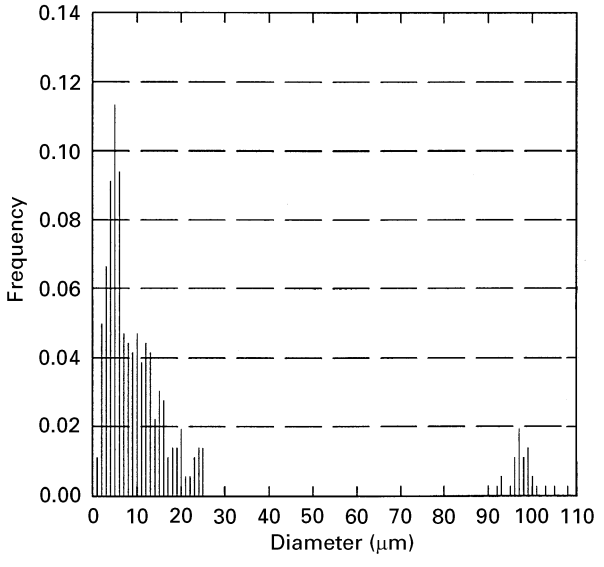

Figure 4 Particle size distribution of HyMu metal ($\phi_m = 0.773$).

3.6. Characterization of magnetic properties

The magnetic permeability measurement setup was designed in accordance with ASTM standard A772-80. The samples were prepared in the form of toroids that were wrapped uniformly with two sets of wire winding. The primary coil was excited with a sine wave from a function generator, Hewlett Packard model 200 CDR. The voltage induced in the secondary coil was measured with a lock-in amplifier, EG&G model 5209. The frequency range of the amplifier was from 0.5 Hz to 120 kHz. More information on our characterization of the electrical and magnetic properties of composite samples can be found elsewhere [20, 21].

4. Results and discussion

4.1. Resistivity

Figs 5 and 6 summarize the results of the resistivity measurements for each composite material at the volume concentrations tested. The volume and surface resistivity values of LDPE were found to be greater than the upper limit that our experimental setup could measure, i.e. greater than 10^{18} Ω-cm and 10^{18} Ω, respectively. Both the surface and volume resistivity values show a precipitous drop with increasing volume concentration of filler. It is evident from Figs 5 and 6 that the LDPE–HyMu composite is more conductive than the other two composites, and shows measurably low resistivity values at the 25% and higher loading levels of filler by volume. This may be attributed to the fact that HyMu metal is intrinsically more conductive than the two ferrites and also that composites with broader particle size distributions tend to percolate at a lower filler content [12]. The volume resistivity values, ρ, of HyMu, NiZn and MnZn fillers are 6.2×10^{-5}, 1×10^{5} and 100 Ω-cm, respectively. Both of the ferrite based composites have measurable resistivity values at the 50% and greater filler contents, however, the volume and surface resistivity values of the NiZn-based composite samples are

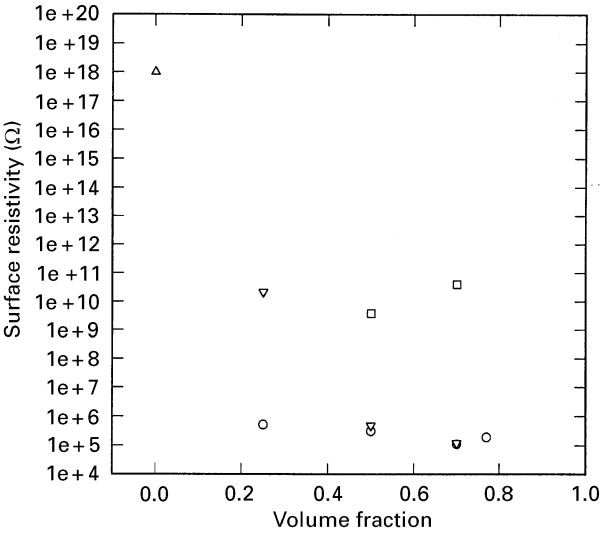

Figure 5 Surface resistivity measured at 1.26 V: (○) HyMu, (□) NiZn, (▽) MnZn, (△) LDPE.

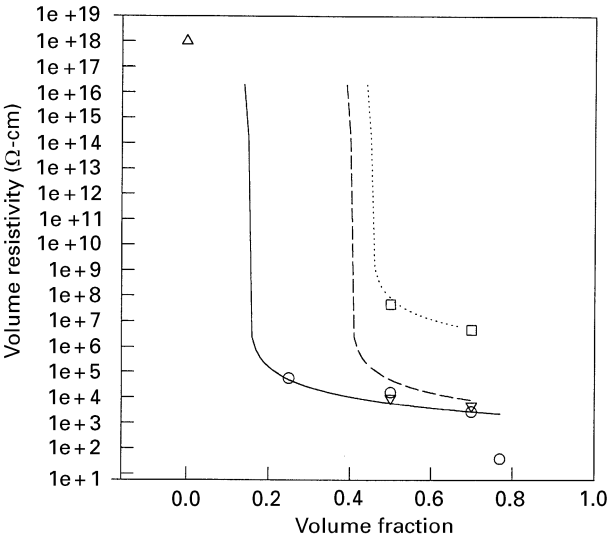

Figure 6 Volume resistivity measured at 1.26V. The intrinsic resistivity values of (○) HyMu metal, (▽) MnZn and (□) NiZn ferrites are 62×10^{-6}, 100 and 10^5 Ω-cm respectively. (△) PE. The lines depict Equation 1: (—) HyMu, (– –) MnZn, (---) NiZn.

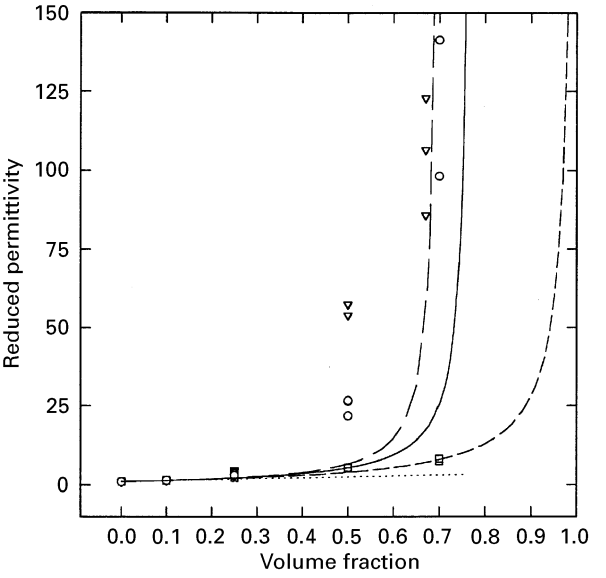

Figure 7 Reduced permittivity measured at 100 kHz: (▽) PE–MnZn, (□) PE–NiZn; (○) PE–HyMu; (—) Equation 7, $\phi_m = 0.77$; (——) Equation 7, $\phi_m = 0.67$; (– –) Equation 7; (----) Equation 4.

orders of magnitude greater than those of the MnZn-based composite. This was expected because the electrical resistivity of NiZn ferrite is several orders of magnitude higher than that of MnZn ferrite (see Fig. 6). For qualitative purposes only, the percolation model of Equation 1, is included in Fig. 6. It is estimated from the data that the ϕ_c parameter of Equation 1, i.e. the best-fit of the critical volume fraction of filler necessary for electrical percolation of LDPE–HyMu composite, is between 0.1 and 0.25 and ϕ_c for LDPE–ferrite composites is between 0.25 and 0.5.

4.2. Dielectric constant versus concentration

The dielectric constant (ratio of the permittivity of the polymer to that of vacuum, $\varepsilon/\varepsilon_0$) of LDPE is 2.2 [3]. The dielectric constant values of composites, $\varepsilon_{eff}/\varepsilon_0$, are known to increase with increasing volume fraction of conductive filler. This is the result of polarization of surface charges induced on the filler particles [17].

The values of the reduced permittivity $\varepsilon_{eff}/\varepsilon$ of the composites are shown in Fig. 7. For comparison, the case of non-interacting spherical particles, Equation 4, is also plotted. The reduced permittivity values of the LDPE–NiZn composite approximately follow Wagner's relationship. This is due to the fact that NiZn ferrite is not a very good conductor, i.e. $\sigma/(\omega\varepsilon) \ll 1$ (where σ is the conductivity and ω is the frequency). On the other hand, the reduced permittivity values of the composites made with good conductors, i.e. HyMu metal and MnZn ferrite, increase two orders of magnitude over that of neat LDPE at the highest concentration levels. At high loading levels (greater than 25%) of LDPE–HyMu and LDPE–MnZn composites the assumption of non-interacting particles is not acceptable. It is apparent from Fig. 7 that there is a non-linear relationship between the permittivity values of these two composites and of the volume fraction of their filler contents. This non-linear permittivity enhancement is caused by higher multiple interactions among the particles that become important when the particles approach each other [22].

It has been shown that when only dipole interactions are important (low loading levels) then the Clausius–Mosotti relation is valid [15]

$$\frac{\varepsilon - 1}{\varepsilon + 2} = \phi \tag{7}$$

The best fit of the Clausius–Mosotti approximation, Equation 7, is shown in Fig. 7. It describes accurately the behaviour of the LDPE–NiZn composite over the 70% volume concentration range. However, it is inadequate for describing the behaviour of the other two composite systems.

Doyle and Jacobs [22] developed an effective cluster model to account for the non-linear dependence of the permittivity on volume concentration. In their model multipole interactions within clusters are treated exactly and external interactions between clusters and isolated spheres are treated with the dipole approximation. The effective polarization per unit volume of the medium, β, is given by

$$\beta = \phi\left[1 + \left(\frac{\phi}{\phi_m}\right)\left(\frac{1}{\phi_m} - 1\right)\right] \tag{8}$$

Here, β becomes unity when $\phi = \phi_m$. This is an improvement over the Clausius–Mosotti condition that permits ϕ to be as high as one, which is not possible. The reduced permittivity is then given by

$$\varepsilon_r = \left(1 + \frac{3\beta}{1 - \beta}\right) \tag{9}$$

The effective cluster model is plotted in Fig. 7 for two cases: $\phi_m = 0.67$ and $\phi_m = 0.77$. The predictions of the effective cluster model agree better with the experimental data at the high solid concentrations for LDPE–HyMu and LDPE–MnZn composites than

the Clausius–Mosotti relationship. The cluster model also predicts that the permittivity values of LDPE–MnZn composite should approach the asymptotic values (metallizaton transition–localized clusters of metal particles) at a lower volume concentration of filler. This is evident at $\phi = 0.5$ where the MnZn composite has a permittivity value that is about twice the value for the HyMu composite.

4.3. Dissipation factor versus concentration

The dissipation factor is defined as the ratio of energy dissipated to that of the energy stored during the reversal of electrical polarization in response to an externally applied alternating electric field. Fig. 8 shows that the dissipation factor of the three composites is a non-linear function of the volume concentration of filler, measured at 100 kHz. The dissipation factor for neat LDPE was measured to be 0.0006. As can be seen from Fig. 8 the dissipation factor increases with increasing volume concentration of filler particles. At the highest loading levels the dissipation factor increased four orders of magnitude over that of neat LDPE. The increase in dissipation factor values with increasing filler concentration was anticipated on the basis of the displacement of surface charges. The displacement contributes to polarization and hence introduces additional losses. The least conductive composite, LDPE–NiZn, exhibits lower losses than the other two composites at the highest loading levels. This behaviour agrees with earlier studies [24].

4.4. Dielectric constant versus frequency

The dielectric constant values for the three composites were determined over a frequency range of 20 Hz to 1 MHz, and are plotted in Figs 9–11. The figures show that the reduced dielectric constant values are frequency dependent, decreasing with increasing frequency. The frequency dependence is more pronounced for higher loading levels, where interparticle charge carrier exchange may occur. As the loading

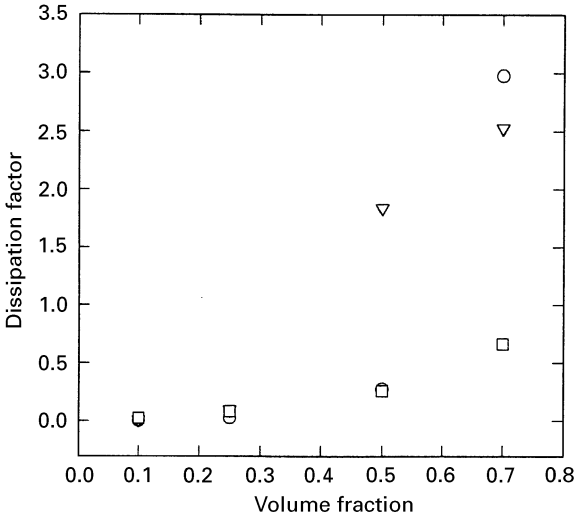

Figure 8 Dissipation factor of composites measured at 100 kHz: (○) HyMu, (□) NiZn, (▽) MnZn.

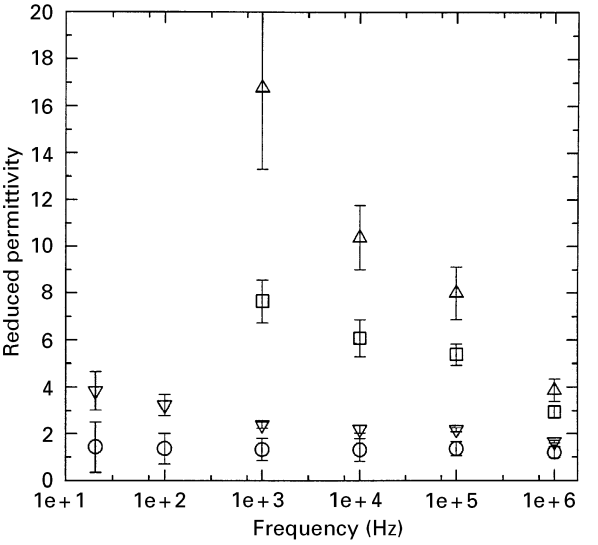

Figure 9 Reduced permittivity of PE–NiZn composites versus frequency at a ratio of 90:10 (○), 75:25 (▽), 50: 50 (□) and 30:70 (△).

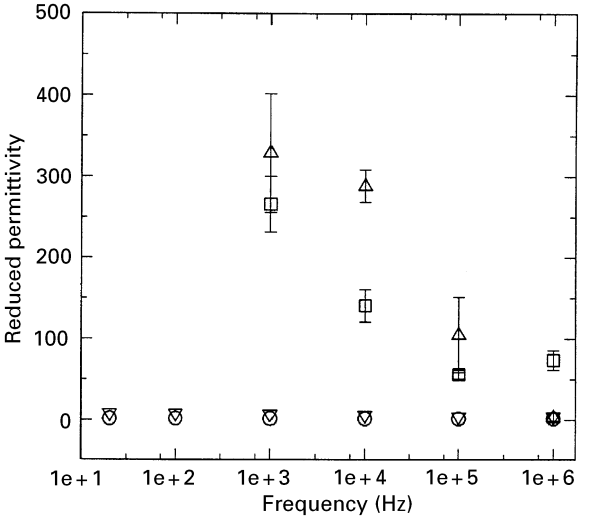

Figure 10 Reduced permittivity of PE–MnZn composites versus frequency at a ratio of 90:10 (○), 75:25 (▽), 50:50 (□) and 33:67 (△).

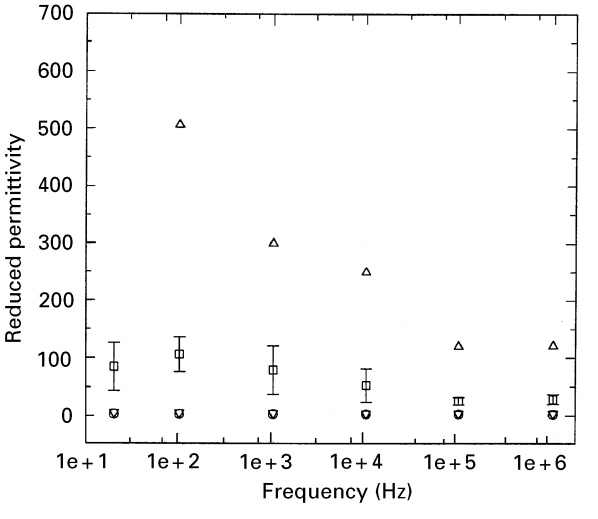

Figure 11 Reduced permittivity of PE–HyMu composites versus frequency at a ratio of 30:70* (△), 50:50 (□), 75:25 (▽) and 90:10 (○) (*mean only).

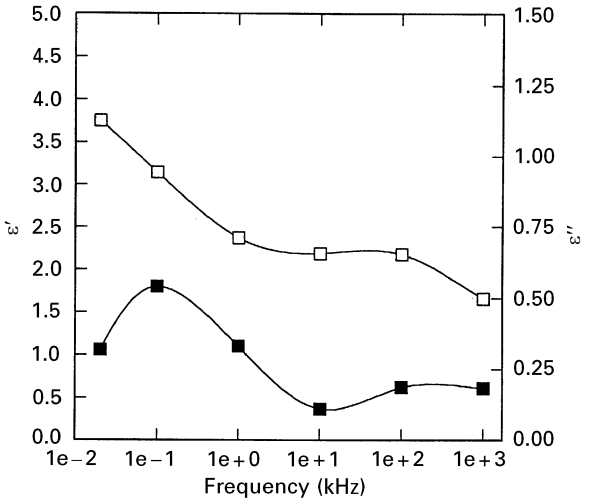

Figure 12 Real ε′ (□), and imaginary ε″ (■), parts of the dielectric constant for LDPE–NiZn 75:25.

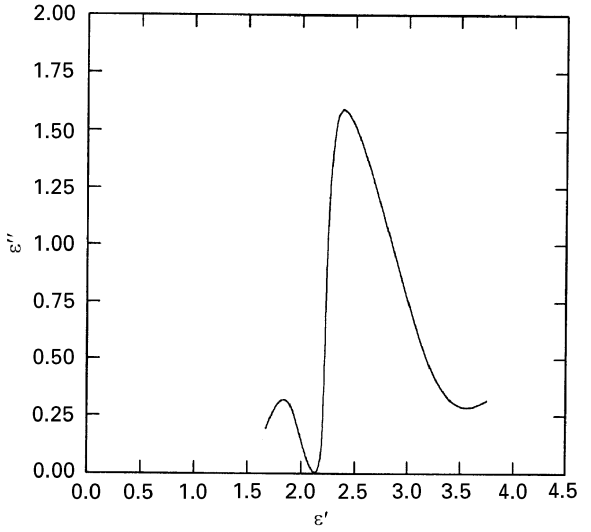

Figure 13 Cole–Cole plot for LDPE–NiZn 75:25.

level increases the clusters become larger and the distances the charge carriers travel become greater. The charges require more time to reorientate, hence the increase in frequency dependence. The composite samples containing 10–25% filler by volume are least sensitive to frequency. This may be attributed to the fact that at this low concentration there is little dielectric enhancement from interfacial polarization, and cluster formation. The concentration is also too low for interparticle interactions.

Fig. 12 shows the real and imaginary parts of the reduced dielectric constant of LDPE–NiZn 75:25 as a function of frequency. The dielectric dispersion appears to be due to multiple polarization mechanisms. The dielectric properties of heterogeneous systems are known to obey the well known Debye equation and will produce a semicircle on Cole–Cole plots [25]. Deviations from the semicircular plot with tails present is an indication that multiple polarization mechanisms may be responsible. Interfacial polarization is known to operate in the lower frequencies where there is more time for the surface charges to reorientate as also supported by the Cole–Cole plot repeated in Fig. 13. The Cole–Cole plots for the other composites were similar to that of LDPE–NiZn. At the higher loading levels the composites gave greatly distorted Cole–Cole circles reflecting different polarization mechanisms with broad distribution of relaxation times occurring from the heterogenous nature of the composites.

4.5. Magnetic permeability versus concentration

The relative magnetic permeability of LDPE is unity due to its inherent non-magnetic nature. As can be seen in Figs 14–16 the magnetic permeability values of the composite samples increase with increasing magnetic filler content. The HyMu filler gives rise to the highest relative permeability value, reaching a value of 26 at volume concentrations that are close to the maximum packing fraction. The greater

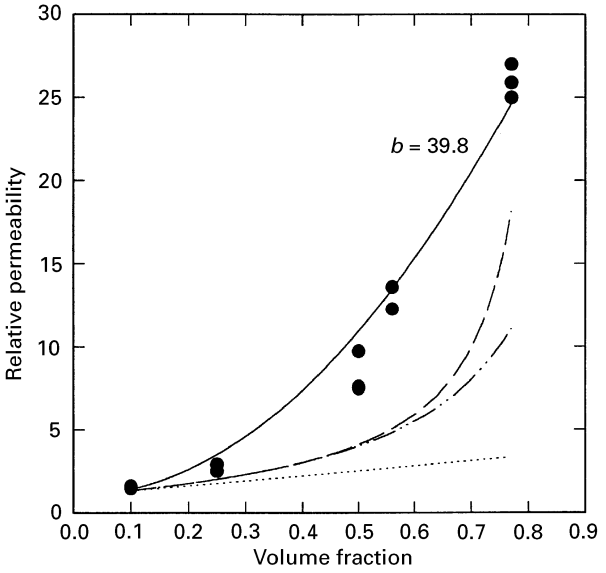

Figure 14 Relative permeability of PE–HyMu composites: (—) $1 + b\phi^2$, (----) Equation 6, (–··–) Equation 10, (– –) Equation 11. HyMu (●) has an intrinsic $\mu_r = 50\,000$.

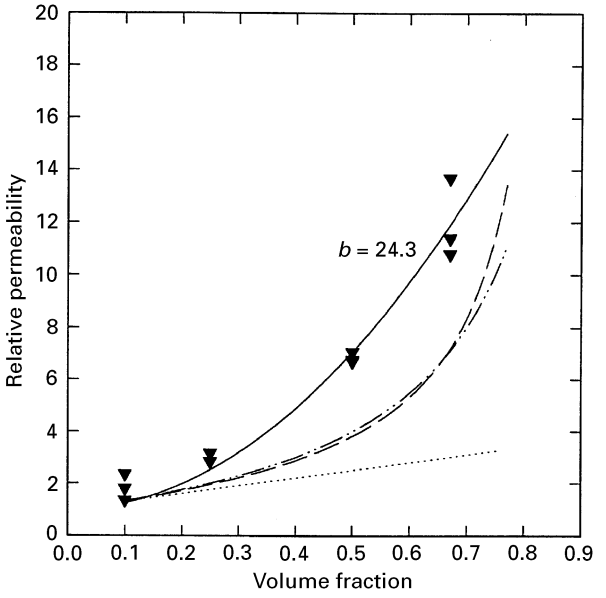

Figure 15 Relative permeability of LDPE–MnZn composites: (—) $1 + b\phi^2$, (----) Equation 6, (–··–) Equation 10, (– –) Equation 11. MnZn (▼) ferrite has an intrinsic $\mu_r = 3000$.

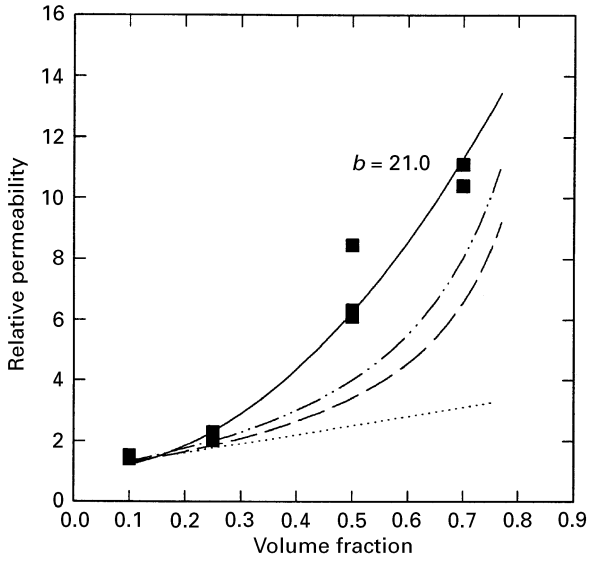

Figure 16 Relative permeability of LDPE–NiZn composites: (—) $1 + b\phi^2$, (- - - -) Equation 6, (— · · —) Equation 10, (– –) Equation 11. NiZn (■) ferrite has an intrinsic $\mu_r = 3000$.

permeability values obtained with HyMu filler are related to the relatively higher intrinsic permeability of HyMu metal, which is two orders of magnitude greater than those of the ferrite fillers. Also, the HyMu powder exhibits a broader particle size distribution allowing for a greater ϕ_m than the other two fillers. However, significant increases in magnetic permeability were observed for all composite samples. Composites incorporated with the two ferrites show relative permeability values that are proportional to the intrinsic permeability values of the ferrites (intrinsic values are of the same order of magnitude).

In addition to the experimental data, the calculated permeability values according to several analytical models were also determined and shown in Figs 14–16. It can be seen in Figs 14–16 that the data deviate significantly from the linear behaviour expected purely on the basis of non-interacting particles, i.e. Equation 6. The deviation from linear dependence on volume fraction of magnetic filler supports the attainment of magnetic percolation. The data thus indicate that particle–particle interactions become important at $\phi > 0.25$.

Hashin and Shtrikman [26] have used a variational approach to determine the upper and lower bounds of the effective magnetic permeability of multiphase materials. They assume that the composite consists of coated spheres, all of which are similar to within a scale factor, i.e. the ratios of the volume of the coated spheres to that of the coating material are similar. They also assume that the composite is densely packed, i.e. they occupy all space by having an infinite size distribution. They have shown that when component 1 coats component 2 ($\mu_2 > \mu_1$) then the effective permeability is given by

$$\mu_{eff} = \mu_1 + \frac{3\phi_2\mu_1(\mu_2 - \mu_1)}{3\mu_1 + \phi_1(\mu_2 - \mu_1)} \tag{10}$$

Equation 10 is plotted in Figs 14–16.

Lam [27] has modelled the effective magnetic permeability of a simple cubic lattice of conducting magnetic spheres. He uses a quasi-static approach (one of the two time derivatives in Maxwell's equations is equated to zero) and includes the eddy current effect. A general expression for the magnetic permeability is given as a series expansion in powers of the volume fraction of the spheres. The effective permeability is given by

$$\frac{\mu_{eff}}{\mu_1} = 1 + \frac{3\phi}{\Lambda} \tag{11}$$

where μ_1 is the permeability of the matrix, and for a simple cubic matrix Λ is given by

$$\Lambda = -\frac{1}{R_1} - \phi + 1.304R_3\phi^{10/3} + 0.0723R_5\phi^{14/3} - 0.5289R_3^2\phi^{17/3} + 0.1526R_7\phi^6 \tag{12}$$

and for a face centred cubic lattice

$$\Lambda = -\frac{1}{R_1} - \phi + 0.0753R_3\phi^{10/3} + 0.242R_5\phi^{14/3} + 0.0558R_3^2\phi^{17/3} + 0.231R_7\phi^6 \tag{13}$$

The constitutive properties of the spheres are contained in the function R_n

$$R_n = \frac{n\mu_1[aj_n(ka)]' - n(n+1)\mu_2 j_n(ka)}{(n+1)\mu_1[(aj_n(ka)]' + n(n+1)\mu_2 j_n(ka)} \tag{14}$$

where μ_2 is the permeability, a is the radius of the spheres; and $ka = (1 + i)(a/\delta)$, where δ represents the skin depth. The j_n represents spherical Bessel function and the prime denotes partial differentiation with respect to a. This model is also plotted in Figs 14–16.

Both the Hashin and Shtrikman [26] and Lam [27] models indicate that the effective permeability of a magnetic composite is a non-linear function of filler volume. However, our experimental data indicate percolation at a lower threshold than predicted by either model.

For each composite a second-order quadratic equation, $1 + b\phi^2$, was fitted to the data. The coefficient, b, is related to the intrinsic magnetic properties of the filler and its shape. Greater values of b indicate larger magnetic enhancement. The HyMu composite showed the largest enhancement with a b value of 39.8, followed by the MnZn and NiZn composites with b values of 24.3 and 21.0, respectively. Overall, the quadratic equation fits the behaviour of all the composites. The non-linear enhancement of magnetic permeability with increasing filler content, especially approaching the maximum packing fraction, ϕ_m, is not as pronounced as those observed for the electrical properties.

4.6. Magnetic permeability versus frequency

The relative permeability of the composite samples were characterized as a function of frequency between

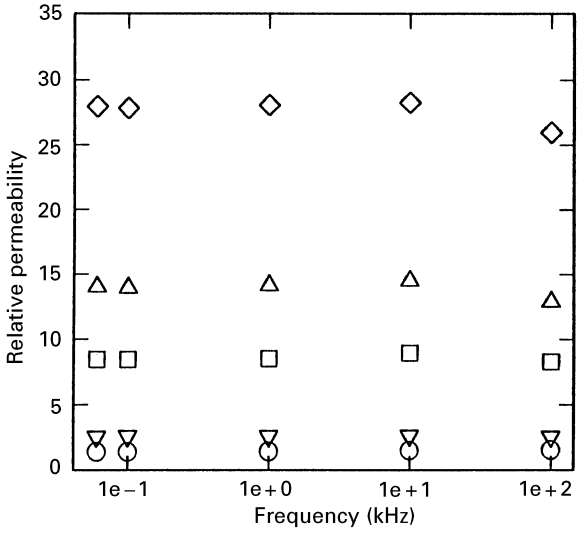

Figure 17 Relative permeability of LDPE–HyMu composites versus frequency for a ratio of 90:10 (○), 75:25 (▽), 50:50 (□), 70:30 (△) and 23:77 (◇).

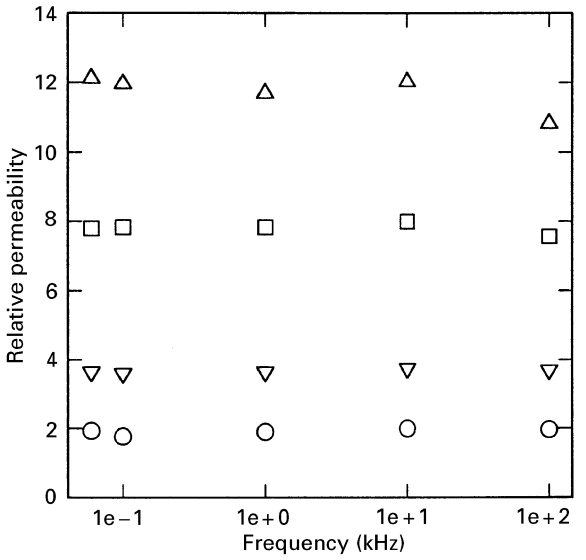

Figure 18 Relative permeability of LDPE–MnZn composites versus frequency for a ratio of 90:10 (○), 75:25 (▽), 50:50 (□), and 33:67 (△).

20 Hz and 0.1 MHz as shown in Figs 17–19. The magnetic permeability remained insensitive to frequency for the three composites except for the highest frequency values around 100 kHz, where the magnetic permeability values decreased in comparison with the values at low frequencies. For most ferromagnetic materials, including ferrites, the permeability values are known to vary with frequency [28, 29]. However, constant magnetic permeability values over a wide frequency range are essential for some applications.

4.7. Percolation

An interesting observation to note is how the trends of the curves are parallel to one another for three of the properties measured for each material. The reduced

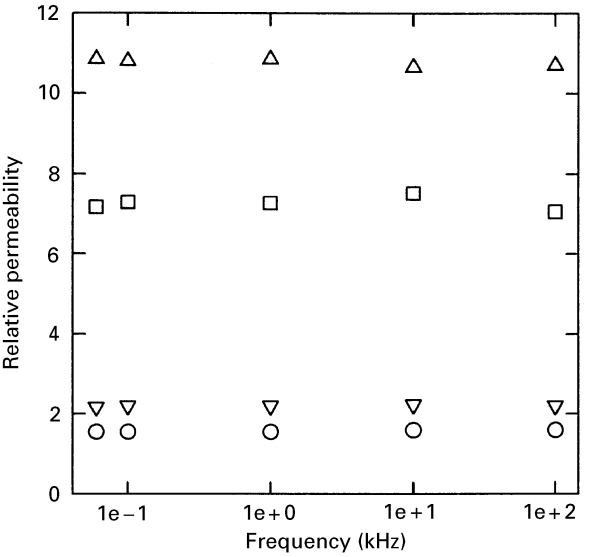

Figure 19 Relative permeability of LDPE–NiZn composites versus frequency for a ratio of 90:10 (○), 75:25 (□), 50:50 (▽), and 33:67 (△).

permittivity, dissipation factor and relative permeability appear to percolate at the same level of filler concentration for each material. As was noted earlier, particle–particle interactions become important above volume fractions greater than 0.2 as is evident from the graphs.

5. Conclusions

The electric and magnetic properties of three types of magnetic composite incorporated with ferromagnetic fillers, i.e. HyMu, MnZn and NiZn ferrites, were characterized. Specifically, volume and surface resistivity, dielectric constant, electric loss factor and relative magnetic permeability behaviour of the composites were determined as a function of the concentration of the magnetic filler.

For all three fillers the volume and surface resistivity values decrease with increasing filler concentration, reaching values that are up to 16 orders of magnitude smaller than those of neat LDPE at loading levels that approach the maximum packing fraction. The dielectric constant values increase with increasing filler content. Particle–particle interactions are significant in affecting the dielectric constant values. The dielectric constant values demonstrate a strong dependency on frequency.

The relative magnetic permeability values increase with increasing volume concentration but are affected only slightly from the frequency over 0.1–100 kHz. The relative magnetic permeability enhancement with increasing filler content was not as drastic as those observed with electric properties. Similar results were obtained in our earlier studies with thermoplastic elastomer composites [7] and low density polyethylene–nickel composites [8]. However, in this study we obtained a relative permeability value that was four times greater than those obtained in our previous studies. Also, we showed a second-order dependency of the permeability with volume fraction of the filler.

References

1. J. M. MARGOLIS, "Conductive polymers and plastics" (Chapman & Hall, New York, 1989).
2. H. S. GOKTURK, T. J. FISKE and D. M. KALYON, SPE ANTEC Technical Papers vol. 38 (SPE, 1992) p. 491.
3. D. M. BIGG, *Adv. Polym. Technol.* **3**/**4** (1984) 255.
4. H. L. HOLBROOK, *Int. J. Powder Met.* **1** (1984) 39.
5. J. M. DADEK, French Patent 1 135 734 (1955).
6. E. P. WOHLFARTH, "Ferromagnetic materials" (North-Holland, New York, 1986).
7. H. S. GOKTURK, T. J. FISKE and D. M. KALYON, *IEEE Trans. Mag.* **29** (1993) 4170.
8. *Idem*, *J. Appl. Polym. Sci.* **50** (1993) 1891.
9. P. J. S. EWEN and J. M. ROBERTSON, *J. Phys D*: *Appl. Phys.* **14** (1981) 2253.
10. P. S. CLARK, J. W. ORTON and A. J. GUEST, *Phys. Rev. B* **18** (1978) 1813.
11. M. E. WEBER and M. R. KAMAL, SPE ANTEC Tech. Papers vol. 39 (SPE, 1993) p. 618.
12. A. M. LYONS, *Polym. Engng. Sci.* **31** (1991) 445.
13. A. T. PONOMARENKO, V. G. SHEVCHENKO and N. S. ENSKOLOPYAN, in "Advances in polymer science", Vol. 96, edited by N. S. Enikolopyan (Springer-Verlag, Berlin, 1990).
14. J. W. ESSAM, *Rep. Prog. Phys.* **143** (1980) 833.
15. J. R. REITZ, F. J. MILFORD and R. W. CHRISTY, "Foundations of electromagnetic theory", 3rd Edn (Reading, MA, 1980).
16. K. LAL and R. PARSHAD, *J. Phys. D*: *Appl. Phys.* **6** (1973) 1788.
17. W. T. DOYLE, *J. Appl. Phys.* **49** (1978) 795.
18. N. OUCHIYAMA and T. TANAKA, *Ind. Engng. Chem. Fundam.* **23** (1988) 490.
19. T. J. FISKE, S. B. RAILKAR and D. M. KALYON, *Powder Tech.* **81** (1994) 57.
20. H. S. GOKTURK, T. J. FISKE and D. M. KALYON, *J. Appl. Phys.* **73** (1993) 5598.
21. *Idem*, SPE ANTEC Tech Papers vol. 39 (SPE, 1993) p. 605.
22. H. B. LEVINE and D. A. McQUARRIE, *J. Chem. Phys.* **49** (1968) 4181.
23. W. T. DOYLE and I. S. JACOBS, *Phys. Rev. B.* **42** (1990) 9319.
24. M. S. AHMAD and A. M. ZIHILIF, *Polym. Comp.* **13** (1992) 53.
25. L. K. H. VAN BEEK, in "Progress in dielectrics", Vol. 7, edited by J. B. Berks and J. Hart (Heywood, London, 1967).
26. Z. HASHIN and S. SHTRIKMAN, *J. Appl. Phys.* **33** (1962) 3125.
27. J. LAM, *ibid.* **66** (1989) 3741.
28. G. Y. CHIN and J. H. WERNICK, in "Ferromagnetic materials", edited by E. P. Wohlfart (North-Holland, New York, 1986) pp. 55–188.
29. R. BOZORTH, "Ferromagnetism" (Van Nostrand, Princeton, NJ, 1968).

Received 31 October 1995
and accepted 10 February 1997